Original Article

Rolandic Cortex Morphology: Magnetic Resonance Imaging-Based Three-dimensional Cerebral Reconstruction Study and Intraoperative Usefulness

Abstract

Background: During brain surgery, the neurosurgeon must be able to identify and avoid injury to the Rolandic cortex. However, when only a small part of the cortex is exposed, it may be difficult to identify the Rolandic cortex with certainty. Despite various advanced methods to identify it, visual recognition remains an important backup for neurosurgeons. The aim of the study was to find any specific morphology pattern that may help to identify the Rolandic cortex intraoperatively. **Materials and Methods:** Magnetic resonance imaging of the brain from patients with various conditions was used to create the three-dimensional cerebral reconstruction images. A total of 216 patients with 371 intact hemispheres were included. Each image was inspected to note the morphology of the Rolandic cortex and the suprasylvian cortex. In addition, other two evaluators exclusively inspected the morphology of the suprasylvian cortex. Their observation results were compared to find the agreements. **Results:** A number of distinctive morphology patterns have been identified at the Rolandic cortex and the suprasylvian cortex including a genu, or a knob at the upper precentral gyrus (pre-CG), an angulation of the lower postcentral gyrus (post-CG), a strip for pars opercularis, a rectangle for the lower pre-CG, and a triangle for the lower post-CG. Combined total and partial agreement of the suprasylvian cortex morphology pattern ranged 60.4%–85.2%. **Conclusion:** The authors have demonstrated the distinctive morphology of the Rolandic cortex and the suprasylvian cortex. This information can provide visual guidance to identify the Rolandic cortex particularly during surgery with limited exposure.

Keywords: *Cerebral cortex, morphology, Rolandic cortex, suprasylvian cortex, three-dimensional reconstruction*

Krishnapundha Bunyaratavej, Piyanat Wangsawatwong

Division of Neurosurgery, Department of Surgery, Faculty of Medicine, Chulalongkorn University and King Chulalongkorn Memorial Hospital, Bangkok, Thailand

Introduction

Rolandic cortex is the region of the brain surrounding the central sulcus, consisting of precentral gyrus (pre-CG) and postcentral gyrus (post-CG). Due to its central location, a significant number of supratentorial operations take place around the Rolandic cortex. During surgery, the neurosurgeon must be able to recognize and avoid injury to the Rolandic cortex as it generally leads to a major neurological deficit. Despite various methods to identify the Rolandic cortex, i.e. cranial landmark,[1-3] functional imaging,[4-7] electrophysiological mapping,[4,8,9] neuronavigation,[10] there are times when these technologies are not feasible or fail to locate the Rolandic cortex. That is when visual recognition can serve as a contingency method.

There are a number of studies describing anatomical details of the Rolandic cortex, however, data on its morphology and variations are still lacking and most previous studies were based on a limited number of cases.[4,11-16] Therefore, the authors sought to study the Rolandic cortex in magnetic resonance imaging (MRI) based three-dimensional cerebral reconstruction (3DCR) images with the aims to analyze their morphology in a larger sample and to find any specific morphology pattern that may help to identify the Rolandic cortex.

Materials and Methods

The authors retrieved MRI data of the patients who underwent brain MRI for various neurological conditions between January 2014 and December

Address for correspondence:
Dr. Krishnapundha Bunyaratavej,
1873 Rama IV Road,
Pathumwan, Bangkok
10330, Thailand.
E-mail: krishnapundha.b@
chulahospital.org

Access this article online

Website: www.asianjns.org

DOI: 10.4103/ajns.ajns_307_21

Quick Response Code:

2017. There were 273 patients, 5 with failed 3DCR due to technical issues, 52 with suboptimal quality 3DCR. These patients were excluded from the analysis. For patients with unilateral cortical surface distortion, only intact hemisphere and patient data were included in the analysis. Of the remaining 216 patients, there were 371 intact hemispheres (left = 185; right = 186) available for the analysis. There were 111 males and 105 females with mean age of 48.3 years (range: 15–89 years). One hundred and fifty-five patients had both hemispheres intact. The diagnosis consisted of brain tumor in 122 (56.5%) patients, vascular lesion in 16 (7.4%) patients, brain abscess in 9 (4.2%) patients, Parkinson's disease in 31 (14.4%) patients, and miscellaneous in 38 (17.6%) patients.

This retrospective study involving human participants was in accordance with the ethical standards of the institutional and national research committee. Separate written informed consent was not required for this retrospective study. The study was approved by the institutional review board (No. 1372/2019 and 1519/2020).

Magnetic resonance imaging acquisition and three-dimensional cerebral reconstruction

Details of acquisition to create 3DCR in this study are as follows: 3 Tesla MRI unit (Ingenia; Philips Medical Systems, Best, The Netherlands) with a 15-channel array head coil, axial T1-weighted turbo field echo sequences, TR/TE 10/5 milliseconds, flip angle = 8°, slice thickness = 1 mm, no gap, matrix size = 320 × 320, field of view = 380 mm × 230 mm, acquired voxel size 1 mm × 1 mm × 1 mm, number of sections = 180, NEX = 1.0.

MRI data were subsequently transferred to the computer platform and 3DCR was created by anatomical reconstruction software (Anatomical mapping version 1.0, Brainlab, Munich, Germany). Reconstruction software allowed for inspection of 3DCR at various perspectives and magnifications with corresponding 3 orthogonal planes of the two-dimensional images.

Interpretation methodology and data collection

The 3DCR images of the Rolandic cortex and the suprasylvian cortex (pars opercularis [Pop], lower pre-CG, and lower post-CG) were inspected by the senior author (KB) to note their characteristics. The Rolandic cortex was identified by a combination of the published methods.[17] By a combination of various methods, the Rolandic cortex was identified with certainty in all hemispheres. The following characteristics were noted: the morphology of the upper pre-CG; the angulation of the lower post-CG [Figure 1a and b].

After the senior author examined a large number of 3DCR images, the common morphology patterns of the suprasylvian cortex were observed as follows:

(1) strip (ST): long cortex narrower than the nearby cortex, (2) rectangle (RT): long cortex with equal or greater width compared to the nearby cortex, (3) triangle (TA): cortex with narrow apex and wide base, (4) unclassified (UC): cortex which does not conform with any of the aforementioned morphology as shown in Figure 1c. In addition, the 3DCR images of the suprasylvian cortex were inspected by two other senior neurosurgical residents who are well-acquainted with cerebral cortex morphology and were blinded to the others' observations. The results from each evaluator were compared, and the evaluator agreement for each part of the suprasylvian cortex was classified into 3 out of 3, 2 out of 3, and no agreement. For each evaluator, the inspection was repeated approximately 2 weeks following the initial inspection to analyze intra-evaluator agreement. For the inter-evaluator agreement, only the results of the initial inspection were analyzed.

Statistical analysis

Descriptive statistics were used to describe patient characteristics and morphology of the Rolandic cortex and the suprasylvian cortex. Cohen's kappa coefficient was used to analyze intra-evaluator agreement. Fleiss' kappa was used to analyze inter-evaluator agreement. Statistical analysis was performed by using IBM SPSS version 28.0 software (IBM Co., Armonk, NY, USA). A $P < 0.05$ was considered statistically significant.

Results

Upper precentral gyrus and postcentral gyrus

The characteristics of the morphology of the upper pre-CG and the angulation of the lower post-CG are presented in Table 1.

Suprasylvian cortex

The distribution of morphology and details of the evaluator agreement for each part of the suprasylvian cortex is shown in Table 2. The histogram showing the evaluator agreement for each morphology category is shown in Figure 2. The individual intra-evaluator reliability was 0.712, 0.652, 0.685 ($P < 0.001$), respectively. The overall inter-evaluator agreement among 3 evaluators was 0.541 (95% confidence interval: 0.520–0.561, $P < 0.001$). Details of inter-evaluator agreement on each morphology pattern are shown in Table 3.

Table 1: Characteristics of the Rolandic cortex

	Left (n=185), n (%)	Right (n=186), n (%)	Both (n=371), n (%)
Upper pre-CG morphology			
Genu	95 (51.4)	99 (53.2)	194 (52.3)
Knob	41 (22.2)	41 (22.0)	82 (22.1)
Flat	49 (26.5)	46 (24.7)	95 (25.6)
Post-CG angulation	124 (67.0)	85 (45.7)	209 (56.3)

CG – Central gyrus

Table 2: Distribution of morphology of the suprasylvian cortex and evaluator agreement

Hemisphere	Evaluator agreement*	Pars opercularis[†] (%)				Lower precentral gyrus[†] (%)				Lower postcentral gyrus[†] (%)			
		ST	RT	TA	UC	ST	RT	TA	UC	ST	RT	TA	UC
Left	3/3	49.2	0	0.5	0	2.7	30.3	1.6	5.4	0.5	2.2	51.4	0.5
(n=185)	2/3	35.7	2.7	0.5	6.5	9.2	24.3	1.6	16.8	5.4	6.5	19.5	7.0
	No agreement	4.9				8.1				7.0			
Right	3/3	62.4	0	0.5	0	0.5	47.8	1.6	1.1	1.6	1.1	55.9	0
(n=186)	2/3	23.1	4.3	0.5	5.9	4.3	18.3	4.3	11.8	4.3	5.4	17.2	7.5
	No agreement	3.2				10.2				7.0			
Both	3/3	55.8	0	0.5	0	1.6	39.1	1.6	3.2	1.1	1.6	53.6	0.3
(n=371)	2/3	29.4	3.5	0.5	6.2	6.7	21.3	3.0	14.3	4.9	5.9	18.3	7.3
	No agreement	4.0				9.2				7.0			

*3/3=3 out of 3 evaluators agreement; 2/3=2 out of 3 evaluators agreement. [†]ST – Strip; RT – Rectangle; TA – Triangle; UC – Unclassified
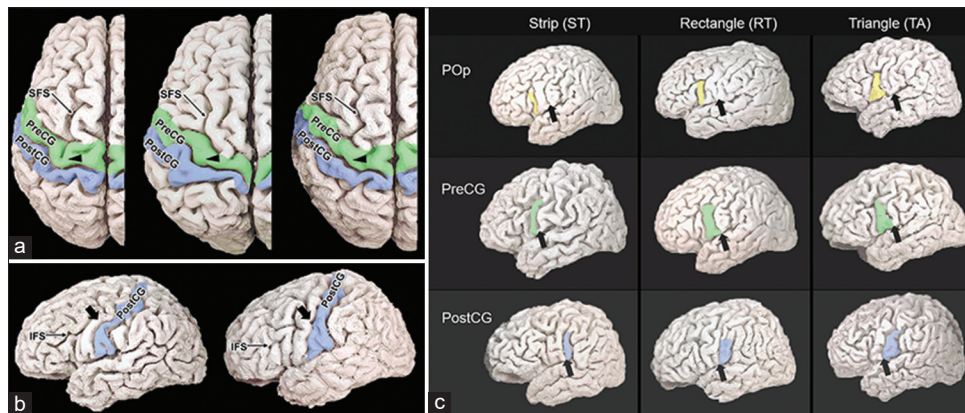

Figure 1: (a) Variations of precentral gyrus (arrowhead). Left: genu; middle: knob; right: flat. (b) Angulation of postcentral gyrus (thick arrow). Left: angle; Right: straight. (c) Variations of the suprasylvian cortex. Central sulcus (thick arrow). IFS = inferior frontal sulcus; SFS = superior frontal sulcus
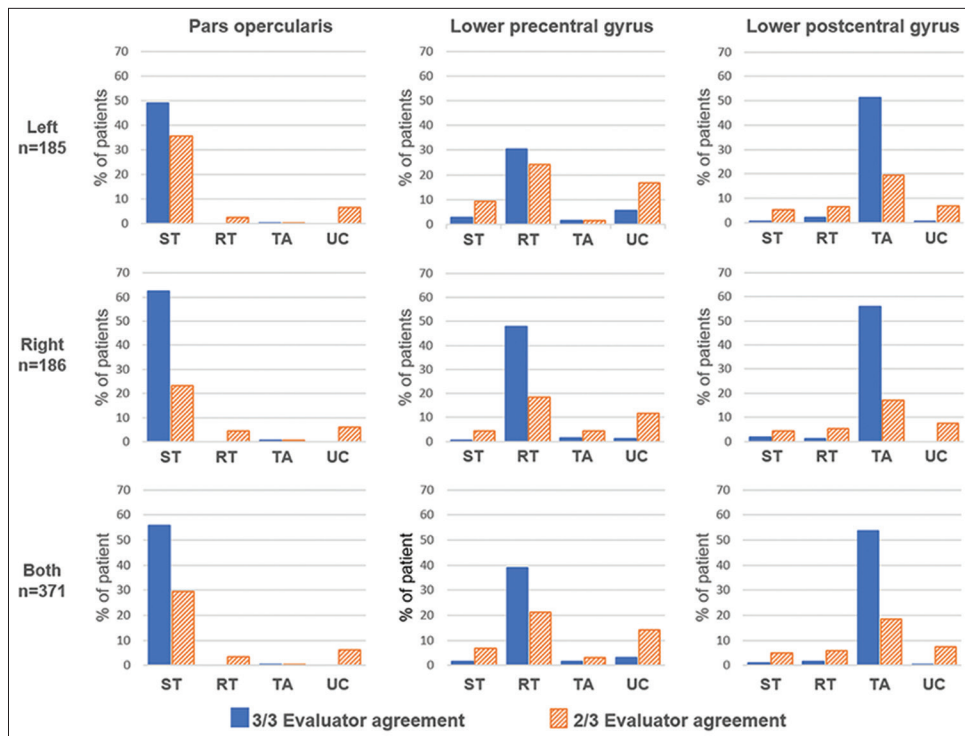

Figure 2: Histograms showing the distribution of the morphology of the suprasylvian cortex for left, right, and both hemispheres. ST = strip; RT = rectangle; TA = triangle; UC = unclassified

Discussion

When the Rolandic cortex is fully exposed as in a cadaveric specimen, it can be readily distinguished from the surrounding cortex by its oblique orientation between the interhemispheric fissure and the mid part of the Sylvian fissure. However, in the operative scenario, only a limited part of the Rolandic cortex is generally visualized. Thus, a number of methods including functional MRI, neuronavigation, electrophysiological mapping, are commonly used to locate the Rolandic cortex.[4-10] Nevertheless, visual recognition remains indispensable knowledge for neurosurgeons and can serve as a backup method when other approaches are not feasible or not successful.

Previous publications focusing on localizing the Rolandic cortex were mostly based on the morphology on the two-dimensional orthogonal planes of an MRI or functional imaging which required navigation system to link the data onto the actual surgical field.[4-6,10,16-21] Publications on the actual morphology of the Rolandic cortex were based on the limited number of cases.[11-15,22]

Data of morphology in our study were based on 371 hemispheres of 3DCR which has been shown to correlate well with the intraoperative findings.[23-27] This large number of samples created an opportunity to encounter variations and uncommon morphology. From our study, we can summarize the surgical anatomy of the Rolandic cortex and the suprasylvian cortex as follows.

Upper precentral gyrus

The morphology of the pre-CG varies from one report to another but the posteriorly directed curvature located at the level of superior frontal sulcus is constantly observed among the publications.[11,14,28,29] This curvature has been consistently shown to control contralateral hand function.[11,13,16,20,21] This structure is not only an important landmark intraoperatively but it is also used to identify central sulcus on an MRI study where it appears as an omega-or epsilon-shaped knob projecting posteriorly from the pre-CG on the axial view.[4,11,16,17,20]

In our study, in addition to a complete genu in 52.3%, the authors also found a posteriorly projected knob and smooth straight gyrus in 22.1% and 25.6% at the upper pre-CG, respectively. Therefore, a genu or a knob may be useful for identifying the pre-CG during surgery around the upper Rolandic cortex. This variation has not been reported previously.

Suprasylvian cortex

The POp, the lower pre-CG, and the lower post-CG were collectively referred to as the suprasylvian cortex. Our study showed that their appearances can be categorized into 4 patterns: ST, TA, RT, and UC. With these categories, our results demonstrated substantial intra-evaluator agreement and moderate inter-evaluator agreement.[30]

This present study also used the percentage of evaluator agreement to identify the morphology pattern of each part of the suprasylvian cortex. The percentage of total evaluator agreement (3 out of 3) represented the frequency of a certain pattern (ST, RT, TA, or UC) that was clearly perceived and agreed upon by all evaluators while the percentage of partial evaluator agreement (2 out of 3) represented the frequency of a certain pattern that was not as unanimously perceived but was still agreed upon by 2 evaluators [Figure 2]. Overall, this study has shown that, for each part of the suprasylvian cortex, one pattern clearly dominated the others whether by considering total agreement (range: 39.1%–55.8%), partial agreement (range: 18.2%–29.4%), or combined total and partial agreement (range: 60.4%–85.2%). This suggests that each part of the suprasylvian cortex possesses a unique morphology pattern as follows.

The POp morphology possessed the highest uniformity among the three parts and was invariably classified as ST with combined total and partial agreements of 85.1% for both hemispheres. It is the most posterior part of the inferior frontal gyrus situated anteriorly adjacent to the pre-CG. Thus, its identification leads to the identification of the Rolandic cortex.

The lower pre-CG was mainly classified as RT, although the lower rate of total agreement and higher UC morphology as compared to the POp and the post-CG. This implies the more heterogeneity of the morphology of this area which makes it less dependable to be used as visual guidance.

The lower post-CG morphology was predominantly classified as TA with combined total and partial agreements of 71.9% for both hemispheres. The triangular shape of the lower post-CG was also observed in the previous study.[12] Moreover, the post-CG turns posteriorly at the level of inferior frontal sulcus as it coursed toward the Sylvian fissure in 56.3% [Table 1].

Case illustration

Case 1

A 46-year-old patient presented with left insular glioma. Operative findings show typical morphology of the 3 parts of suprasylvian cortex; POp (ST), pre-CG (RT), and post-CG (TA) with the angulation. The Rolandic cortex can be readily identified based on the morphology [Figure 3].

Case 2

A 19-year-old patient presented with left inferior frontal tumor. Operative findings show typical morphology of the lower post-CG (TA) with angulation at its apex and posteriorly projected genu at the upper pre-CG. Despite the tumor, the morphology is still preserved and can be used to identify the Rolandic cortex [Figure 4].
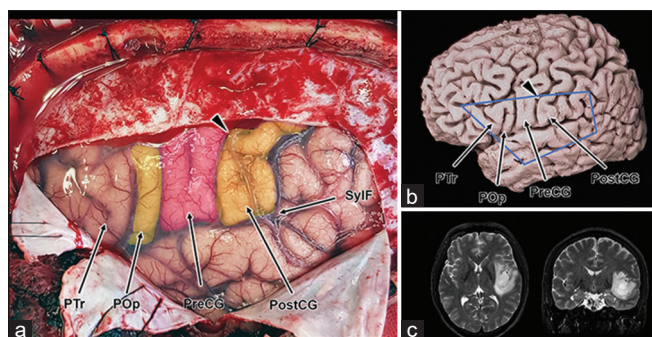
Figure 3: Case 1. (a) Operative photograph revealing morphology of the suprasylvian cortex. Note the angulation of the lower postcentral gyrus (arrowhead). (b) Patient's three-dimensional cerebral reconstruction. (c) Magnetic resonance imaging. PTr = pars triangularis; SylF = Sylvian fissure

Figure 4: Case 2. (a) Morphology of the suprasylvian cortex as follows: strip for POp; triangle for the lower postcentral gyrus with the angulation (arrowhead). Note genu at the upper precentral gyrus. (b) Patient's three-dimensional cerebral reconstruction. (c) Magnetic resonance imaging. SylF = Sylvian fissure
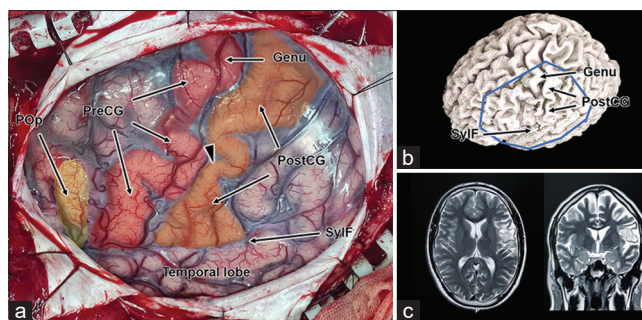
Table 3: Inter-evaluator agreement

Morphology pattern	Kappa	95% CI	*P*
ST	0.587	0.553-0.621	<0.001
RT	0.590	0.556-0.624	<0.001
TA	0.679	0.645-0.713	<0.001
UC	0.166	0.132-0.200	<0.001
Overall	0.541	0.520-0.561	<0.001

ST – Strip; RT – Rectangle; TA – Triangle; UC – Unclassified; CI – Confidence interval

These illustrative cases demonstrated that the distinctive appearance can help identify the Rolandic cortex and that the presence of brain tumor or mass effect does not necessarily preclude the use of this morphology to identify the Rolandic cortex.

Important findings derived from our study include: (1) authors have identified various characteristics which are agreeable by multievaluators and these characteristics can be used to directly or indirectly identify the Rolandic cortex. (2) A large sample size created greater opportunities to identify the distribution of common characteristics as well as uncommon morphological variations, some of which have not been previously reported.

However, there are some limitations worth mentioning. First, marked cortical distortion from the pathologic process may render the identification difficult. Moreover, thick and hazy arachnoid membrane or sizable cortical vessels may obscure the sulcal and gyral patterns and hinder correct identification of the underlying cortex. In addition, morphologic study certainly carries inherent ambiguity of the interpretation even with repeated tests of the multiple evaluators. Finally, correct identification of the Rolandic cortex does not guarantee functional preservation. Individual variation of motor and sensory function is well established. These functions occasionally extend beyond the Rolandic cortex particularly when the lesion is located close to the Rolandic cortex.[9,20,21,31]

Conclusion

The authors have demonstrated distinctive morphology as well as variations of the Rolandic cortex and the suprasylvian cortex by MRI-based 3DCR study. This information can provide visual guidance to identify the Rolandic cortex intraoperatively.

Conflicts of interest

There are no conflicts of interest.

References

1. Ebeling U, Rikli D, Huber P, Reulen HJ. The coronal suture, a useful bony landmark in neurosurgery? Craniocerebral topography between bony landmarks on the skull and the brain. Acta Neurochir (Wien) 1987;89:130-4.
2. Kendir S, Acar HI, Comert A, Ozdemir M, Kahilogullari G, Elhan A, et al. Window anatomy for neurosurgical approaches. Laboratory investigation. J Neurosurg 2009;111:365-70.
3. Sarmento SA, Jacome DC, de Andrade EM, Melo AV, de Oliveira OR, Tedeschi H. Relationship between the coronal suture and the central lobe: how important is it and how can we use it in surgical planning? Arq Neuropsiquiatr 2008;66:868-71.
4. Lehericy S, Duffau H, Cornu P, Capelle L, Pidoux B, Carpentier A, et al. Correspondence between functional magnetic resonance imaging somatotopy and individual brain anatomy of the central region: comparison with intraoperative stimulation in patients with brain tumors. J Neurosurg 2000;92:589-98.
5. Pujol J, Deus J, Acebes JJ, Villanueva A, Aparicio A, Soriano-Mas C, et al. Identification of the sensorimotor cortex with functional MRI: frequency and actual contribution in a neurosurgical context. J Neuroimaging 2008;18:28-33.
6. Rao SM, Binder JR, Hammeke TA, Bandettini PA, Bobholz JA, Frost JA, et al. Somatotopic mapping of the human primary motor cortex with functional magnetic resonance imaging. Neurology 1995;45:919-24.

7. Sanchez-Panchuelo RM, Francis S, Bowtell R, Schluppeck D. Mapping human somatosensory cortex in individual subjects with 7T functional MRI. J Neurophysiol 2010;103:2544-56.

8. Farrell DF, Burbank N, Lettich E, Ojemann GA. Individual variation in human motor-sensory (rolandic) cortex. J Clin Neurophysiol 2007;24:286-93.

9. Uematsu S, Lesser R, Fisher RS, Gordon B, Hara K, Krauss GL, et al. Motor and sensory cortex in humans: topography studied with chronic subdural stimulation. Neurosurgery 1992;31:59-71.

10. Jannin P, Morandi X, Fleig OJ, Le Rumeur E, Toulouse P, Gibaud B, et al. Integration of sulcal and functional information for multimodal neuronavigation. J Neurosurg 2002;96:713-23.

11. Boling W, Olivier A, Bittar RG, Reutens D. Localization of hand motor activation in Broca's pli de passage moyen. J Neurosurg 1999;91:903-10.

12. Boling W, Reutens DC, Olivier A. Functional topography of the low postcentral area. J Neurosurg 2002;97:388-95.

13. Boling WW, Olivier A. Localization of hand sensory function to the pli de passage moyen of Broca. J Neurosurg 2004;101:278-83.

14. Frigeri T, Paglioli E, de Oliveira E, Rhoton AL, Jr. Microsurgical anatomy of the central lobe. J Neurosurg 2015;122:483-98.

15. Ribas GC, Yasuda A, Ribas EC, Nishikuni K, Rodrigues AJ, Jr. Surgical anatomy of microneurosurgical sulcal key points. Neurosurgery 2006;59:ONS177-210.

16. Yousry TA, Schmid UD, Alkadhi H, Schmidt D, Peraud A, Buettner A, et al. Localization of the motor hand area to a knob on the precentral gyrus. A new landmark. Brain 1997;120:141-57.

17. Wagner M, Jurcoane A, Hattingen E. The U sign: tenth landmark to the central region on brain surface reformatted MR imaging. AJNR Am J Neuroradiol 2013;34:323-6.

18. Berger MS, Cohen WA, Ojemann GA. Correlation of motor cortex brain mapping data with magnetic resonance imaging. J Neurosurg 1990;72:383-7.

19. Bittar RG, Olivier A, Sadikot AF, Andermann F, Pike GB, Reutens DC. Presurgical motor and somatosensory cortex mapping with functional magnetic resonance imaging and positron emission tomography. J Neurosurg 1999;91:915-21.

20. Bittar RG, Olivier A, Sadikot AF, Andermann F, Reutens DC. Cortical motor and somatosensory representation: effect of cerebral lesions. J Neurosurg 2000;92:242-8.

21. Yousry TA, Schmid UD, Jassoy AG, Schmidt D, Eisner WE, Reulen HJ, et al. Topography of the cortical motor hand area: prospective study with functional MR imaging and direct motor mapping at surgery. Radiology 1995;195:23-9.

22. Ribas GC, Ribas EC, Rodrigues CJ. The anterior sylvian point and the suprasylvian operculum. Neurosurg Focus 2005;18:E2.

23. Bunyaratavej K, Siwanuwatn R. Three-Dimensional Cortical Surface Reconstruction Versus Operative Findings: Their Similarity and Applications. World Neurosurg 2017;107:809-19.

24. Chabrerie A, Ozlen F, Nakajima S, Leventon ME, Atsumi H, Grimson E, et al. Three-dimensional image reconstruction for low-grade glioma surgery. Neurosurg Focus 1998;4:e7.

25. Hu XP, Tan KK, Levin DN, Galhotra S, Mullan JF, Hekmatpanah J, et al. Three-dimensional magnetic resonance images of the brain: application to neurosurgical planning. J Neurosurg 1990;72:433-40.

26. Kikinis R, Gleason PL, Moriarty TM, Moore MR, Alexander E, 3rd, Stieg PE, et al. Computer-assisted interactive three-dimensional planning for neurosurgical procedures. Neurosurgery 1996;38:640-9.

27. Zele T, Matos B, Knific J, Bajrovic FF, Prestor B. Use of 3D visualisation of medical images for planning and intraoperative localisation of superficial brain tumours: our experience. Br J Neurosurg 2010;24:555-60.

28. Rhoton AL, Jr. The cerebrum. Neurosurgery 2002;51:S1-51.

29. Ribas GC. The cerebral sulci and gyri. Neurosurg Focus 2010;28:E2.

30. Landis JR, Koch GG. The measurement of observer agreement for categorical data. Biometrics 1977;33:159-74.

31. Nii Y, Uematsu S, Lesser RP, Gordon B. Does the central sulcus divide motor and sensory functions? Cortical mapping of human hand areas as revealed by electrical stimulation through subdural grid electrodes. Neurology 1996;46:360-7.